Published in final edited form as:
Biochemistry. 2012 July 24; 51(29): 5774–5783. doi:10.1021/bi300530x.

FTIR Study of the Photoactivation Process of *Xenopus* (6-4) Photolyase†

Daichi Yamada[‡], **Yu Zhang**[‡], **Tatsuya Iwata**[‡,§], **Kenichi Hitomi**[∥,⊥], **Elizabeth D. Getzoff**[∥], and **Hideki Kandori**[‡,*]

[‡]Department of Frontier Materials, Nagoya Institute of Technology, Showa-ku, Nagoya, 466-8555, Japan

[§]Center for Fostering Young and Innovative Researchers, Nagoya Institute of Technology, Showa-ku, Nagoya 466-8555, Japan

[∥]Department of Molecular Biology and the Skaggs Institute for Chemical Biology, The Scripps Research Institute, La Jolla, CA 92037

[⊥]Section of Laboratory Equipment, National Institute of Biomedical Innovation, 7-6-8, Saito-Asagi, Ibaraki, Osaka 567-0085, Japan

Abstract

Photolyases (PHRs) are blue-light activated DNA repair enzymes that maintain genetic integrity by reverting UV-induced photoproducts into normal bases. The FAD chromophore of PHRs has four different redox states: oxidized (FAD^{ox}), anion radical ($FAD^{\bullet -}$), neutral radical ($FADH^{\bullet}$) and fully reduced ($FADH^{-}$). We combined difference Fourier-transform infrared (FTIR) spectroscopy with UV-visible spectroscopy to study the detailed photoactivation process of *Xenopus* (6-4) PHR. Two photons produce the enzymatically active, fully reduced PHR from oxidized FAD: FAD^{ox} is converted to semiquinone via light-induced one-electron and one-proton transfers, and then to $FADH^{-}$ by light-induced one-electron transfer. We successfully trapped $FAD^{\bullet -}$ at 200 K, where electron transfer occurs, but proton transfer does not. UV-visible spectroscopy following 450-nm illumination of FAD^{ox} at 277 K defined the $FADH^{\bullet}$/$FADH^{-}$ mixture and allowed calculation of difference FTIR spectra among the four redox states. The absence of a characteristic C=O stretching vibration indicated that the proton donor is not a protonated carboxylic acid. Structural changes in Trp and Tyr are suggested from UV-visible and FTIR analysis of $FAD^{\bullet -}$ at 200 K. Spectral analysis of amide-I vibrations revealed structural perturbation of the protein's β-sheet during initial electron transfer ($FAD^{\bullet -}$ formation), transient increase in α-helicity during proton transfer ($FADH^{\bullet}$ formation) and reversion to the initial amide-I signal following subsequent

†This work was supported by grants from Japanese Ministry of Education, Culture, Sports, Science, and Technology to H. K. (20050015, 20108014), and NIH grant GM37684 to E. D. G.. K. H. was supported by the Skaggs Institute for Chemical Biology.

*To whom correspondence should be addressed: Department of Frontier Materials, Nagoya Institute of Technology, Showa-ku, Nagoya 466-8555, Japan. Phone and fax: 81-52-735-5207. kandori@nitech.ac.jp.

SUPPORTING INFORMATION AVAILABLE

FTIR spectral comparison of the present His-tagged sample in this study, and the previous sample preparation using GST-tag[13] for photoactivation and photorepair process (Figure S1), Estimate of the possible involvement of $FADH^{\bullet}$ as the product upon formation of $FAD^{\bullet -}$ at 200 K in Figure 4 (Figure S2), Expanded Figure 5 at 1800-1350 cm^{-1} (Figure S3). This material is available free of charge via the Internet at http://pubs.acs.org.

electron transfer ($FADH^-$ formation). Consequently, in (6-4) PHR, unlike cryptochrome-DASH, formation of enzymatically active $FADH^-$ did not perturb α-helicity. Protein structural changes in the photoactivation of (6-4) PHR are discussed on the basis of the present FTIR observations.

UV components of sunlight are harmful to life, by triggering various chemical reactions inside cells. Organisms have developed diverse defense systems. Photolyases (PHRs)[1] are unique DNA repair enzymes that maintain genetic integrity by reverting UV-induced photoproducts on DNA strands into normal bases with blue light.[1,2] Most prokaryotes have a single PHR that specifically repairs cyclobutane pyrimidine dimer (CPD), whereas some higher eukaryotes possess an additional PHR that restores pyrimidine-pyrimidone (6-4) photoproduct ((6-4) PP) to parental bases. The discovery of (6-4) PHR occurred 40 years after the first isolation of a CPD PHR gene.[3] Due to the greater structural complexity of (6-4) PP compared to CPD, the synthesis of DNA oligonucleotide substrates carrying a single (6-4) PP was more difficult. However, structural determination of (6-4) PHR provides insights into product recognition by the enzyme.[4,5]

The structures of (6-4) PHRs show an overall fold similar to that of CPD PHRs, consisting of α/β and α barrel domains connected with a unique long loop.[4,5] Flavin adenine dinucleotide (FAD) is the common chromophore for both PHRs. The chromophore is buried in the α barrel domain with the redox-active isoalloxazine ring sequestered from solvent. Reduced FAD is the active form for PHR catalysis. The oxidized FAD is a resting state in purified enzymes for (6-4) PHRs[6], while most CPD PHRs stabilize $FADH^{\bullet}$.[1] Remarkably, PHRs have a system to regain activity. In the presence of reducing agent, buried FADs inside PHRs can be light-dependently reduced. PHRs have the tryptophan triad chain, considered important for this photoreduction, that links FAD to the protein surface. In *E. coli* CPD PHR, substitution of the outside tryptophan of the triad chain disturbs this process.[7,8] (6-4) PHRs structurally conserve the tryptophan triad chain with some modification. Two photons are needed for this photactivation: the oxidized form of FAD is first converted to the semiquinone by light-induced one electron and one proton transfers, then to the reduced form $FADH^-$ by light-induced one electron transfer. When the reduced enzyme absorbs another photon in the presence of the (6-4) PP, electron transfer from $FADH^-$ to the photoproduct initiates the repair process.[6,9]

Light-induced difference Fourier-transform infrared (FTIR) spectroscopy is a powerful, sensitive and informative method to study structure-function relationships in photoreceptive proteins.[10–12] Recently, we applied FTIR spectroscopy to full-length *Xenopus laevis* (6-4) PHR and authentic DNA carrying a single (6-4) PP to gain insights into the reaction mechanisms.[13] Consequently, we successfully obtained difference FTIR spectra that correspond to the photoactivation (light-induced FAD reduction) process and light-dependent DNA repair reactions of (6-4) PHR. In addition, time-dependent illumination of samples with different enzyme:substrate stoichiometries distinguished signals characteristic

[1]Abbreviations: PHR, photolyase; CPD, cyclobutane pyrimidine dimmer; (6-4) PP, (6-4) photoproduct; FAD, flavin adenine dinucleotide; FTIR, Fourier transform infrared; FAD^{ox}, fully oxidized form of FAD; $FADH^-$, fully reduced form of FAD; $FADH^{\bullet}$, neutral semiquinoid form of FAD; $FAD^{\bullet-}$, anion radical form of FAD; CRY, cryptochrome; UV–visible, ultraviolet–visible; DTT, dithiothreitol.

of structural changes in the protein and the DNA resulting from binding and catalysis. This opened a new understanding of the molecular mechanisms of (6-4) PHR in atomic detail, particularly on the enzymatic catalysis.

It should be however noted that the reported difference FTIR spectrum of photoactivation is only between fully oxidized (FAD^{ox}) and fully reduced ($FADH^{-}$) forms. On the other hand, the photoactivation process of (6-4) PHR is more complex, where two photons are needed from FAD^{ox}, a resting state. FAD^{ox} is first converted to $FADH^{\bullet}$ by light-induced one electron and one proton transfers (proton-transfer coupled electron transfer; PCET), and then to $FADH^{-}$ by light-induced one electron transfer.[6] This indicates the presence of semiquinoid neutral radical ($FADH^{\bullet}$) as an intermediate. In addition, if electron and proton transfer reaction is separated in the primary PCET, an anion radical intermediate ($FAD^{\bullet-}$) may be captured. This actually happens for insect cryptochrome, in which $FAD^{\bullet-}$ is stable even at room temperature.[14] It is known that the nearest amino acid to the N_5 position of FAD is the determinant of the stability of $FAD^{\bullet-}$, and insect cryptochrome (CRY) has Cys at this position.[15] Most PHR/CRY possess Asn or Asp, where $FAD^{\bullet-}$ is unstable and $FADH^{\bullet}$ is easily formed. It is likely that hydrogen-bonding network anchored by Asn or Asp in this vicinity acts for efficient proton transfer to FAD.[16] In CRY-DASH from *Synechocystis*,[17] mutation of the corresponding Asn to Cys stabilized $FAD^{\bullet-}$.[18] *Xenopus* (6-4) PHR also possesses Asn at this position, and lack of observation of $FAD^{\bullet-}$ at room temperature (Figure 2) is predicted. Here we studied the detailed activation process of *Xenopus* (6-4) PHR, i.e. from FAD^{ox} to $FADH^{-}$, using UV-visible and FTIR spectroscopy. By selecting temperature and illumination wavelength, we are able to obtain difference FTIR spectra of each of four redox states; FAD^{ox}, $FAD^{\bullet-}$, $FADH^{\bullet}$, and $FADH^{-}$.

MATERIALS AND METHODS

Sample Preparation

In our previous paper, *Xenopus* (6-4) PHR was expressed in *E. coli* as a fusion protein with glutathione-*S*-transferase (GST) at the N-terminus, which was cleaved with thrombin after the purification by glutathione sephrose 4B resin (GE Healthcare).[13,19] However, the purified protein amount was low (purified protein: 0.26 mg from 1 L culture), which is disadvantageous for our future study using isotope-labeling and mutation. Therefore, we used His-tag system in this study as follows.

The gene of *Xenopus* (6-4) PHR containing His-tag at the N-terminus was inserted at the NdeI and XhoI sites of the pET-28a expression vector (Novagen). *E. coli* BL21(DE3) transformed with the vector was added to 1 liters of LB medium in a 3-liter flask and grown at 25 °C until $O.D._{660}$ being 1.25-1.5. The culture was then adjusted to 1 mM isopropyl β-D-thiogalactopyranoside, incubated for 24 h, and then harvested by centrifugation. The pellet was frozen at −80 °C, thawed, resuspended in lysis buffer (50 mM sodium phosphate, 200 mM NaCl, and 5 mM imidazole, pH 8.0), and sonicated. Cell debris was removed from the lysate by ultracentrifugation at 17,700 rpm for 1 h. The cell-free extract was loaded onto a TALON Metal Affinity Resin column (TAKARA), and the fusion protein was eluted with elution buffer (50 mM sodium phosphate, 200 mM NaCl, and 500 mM imidazole, pH 8.0). The sample was then applied to a HiTrap Heparin HP column (GE Healthcare) and eluted

with a linear gradient of 0.2-1 M NaCl. The protein expressed in *E. coli* does not bind second chromophore, such as MTHF.[6] A 5-liter culture of *E. coli* yielded 11 mg of (6-4) PHR, which is 8.5-times larger than the previous preparation method using the GST-tag system. When the purified (6-4) PHR was stored, it was kept at −80 °C in 50 mM Tris-HCl buffer (pH 8.0) containing 200 mM NaCl and 5 % (w/v) glycerol.

We used redissolved samples for UV-visible and FTIR spectroscopy, as established in the previous study.[13] First, we put 2 μL of the sample solution containing 1 mM (6-4) PHR in 50 mM Tris-HCl buffer (pH 8.0) and 200 mM NaCl on an IR window (BaF_2), and dried. We then put 0.4 μL of the 50 mM Tris-HCl buffer (pH 8.0) containing 200 mM NaCl directly onto the dried film, and sandwiched by another IR window. (6-4) PHR in D_2O was prepared by diluting the (6-4) PHR with the same buffer prepared in D_2O and concentrating by Amicon YM-30 device (Millipore) for three times. Same procedure was carried out except for using D_2O buffer for the preparation of redissolved samples.

UV-visible and FTIR spectroscopy

UV-visible and FTIR spectra of the redissolved samples were measured using V-550DS (JASCO) and FTS-7000 (DIGILAB) spectrophotometers, respectively, as reported previously.[13,19–21] Samples were placed in an Oxford Optistat-DN cryostat mounted in the spectrophotometer, which was also equipped with a temperature controller (ITC-4, Oxford). The illumination source was a high power 300 W xenon lamp (MAX-302, ASAHI SPECTRA), and illuminations at 450 nm (MZ0450, ASAHI SPECTRA), >550 nm (XF593, ASAHI SPECTRA), 300-400 nm (C-40B, Toshiba) or at >450 nm (VY-45, Toshiba) were provided. The FTIR spectra were constructed from 128 interferograms with spectral resolution of 2 cm^{-1}. The difference spectrum was calculated by subtracting the spectrum recorded before illumination from the spectrum recorded after illumination. Six to eight difference spectra obtained in this way were averaged for each difference spectrum.

In this study, the N-terminal His tag was not removed, and we thus tested whether the His-tagged *Xenopus* (6-4) PHR provides similar spectra to the previous report.[13] Figure S1 compares light-induced difference FTIR spectra of the His-tagged *Xenopus* (6-4) PHR in this study (red line) with the reported spectra (black line) for the photoactivation (Figure S1a; $FADH^-$ minus FAD^{ox}) and for the photorepair (Figure S1b; repaired DNA minus (6-4) PP). Red and black spectra coincide well, and the reproduced spectra demonstrate identical structural changes for the two different preparations.

RESULTS

Capturing $FADH^\bullet$: Light-Induced Difference UV-visible and FTIR Spectra of (6-4) PHR at 277 K

We previously illuminated the redissolved sample of FAD^{ox}, the resting state of (6-4) PHR, with >450-nm light, and obtained $FADH^-$ at 277 K.[13] Under such photoactivation conditions, we did not detect significant absorption near 600 nm, characteristic of $FADH^\bullet$. In contrast, we observed the appearance of a broad absorption at 500-700 nm at 277 K by illuminating FAD^{ox} of (6-4) PHR (redissolved sample) for 4 min at 450 nm, by using an

interference filter (Figure 2a). This clearly shows formation of $FADH^{\bullet}$ at 277 K.[22] It should be noted that the photoproduct is not only $FADH^{\bullet}$, but also $FADH^{-}$. On the other hand, the absence of the $FAD^{\bullet -}$ specific 350-400-nm bands on the positive side implies no accumulation of $FAD^{\bullet -}$.[14] Thus, the result of Figure 2a can be interpreted as follows; illumination converts FAD^{ox} into $FADH^{\bullet}$ by coupled electron and proton transfer reactions, with some species being further reduced to $FADH^{-}$. According to the extinction coefficients of various redox states of *Xenopus* (6-4) PHR reported by Schleicher et al.[22], relative absorbances of 1, 0.54, and 0.24 at 450 nm, and 0, 0.40, and 0 at 580 nm were determined for FAD^{ox}, $FADH^{\bullet}$, and $FADH^{-}$, respectively. From these values, we estimated the positive components of the spectrum in Figure 2a to be 49 % $FADH^{\bullet}$ and 51 % $FADH^{-}$. These values will be used to obtain the “pure” difference FTIR spectra below.

After the spectrum of Figure 2a was obtained by a 450-nm light illumination, we continuously illuminated the sample for 1 min with >550-nm light, which is only absorbed by $FADH^{\bullet}$ (Figure 2b).[22] As the result, $FADH^{\bullet}$ is photoconverted as evidenced by negative broad band at 500–700 nm. FAD^{ox} is involved neither as the reactant nor product, as seen from the absence of its characteristic peaks at 448 and 475 nm in Figure 2b. It is likely that $FADH^{\bullet}$ is dominantly converted into $FADH^{-}$ by an electron transfer.[7] This interpretation is further supported by the spectral analysis in Figure 2c. The sum of the two spectra in Figure 2a and b (red line in Figure 2c) coincides very well with the $FADH^{-}$ minus FAD^{ox} spectrum (black line in Figure 2c) obtained by illuminating FAD^{ox} by >450 nm light. Both spectra agree with the reported $FADH^{-}$ minus FAD^{ox} spectrum.[13] It should be noted that visible absorption at 500–700 nm is characteristic of cation or neutral radicals of Trp and Tyr,[23–25] as well as flavins. However, such signals are not apparent in the present static measurements at 277 K, as evident from the $FADH^{-}$ minus FAD^{ox} spectrum coinciding with the baseline at >500 nm (Figure 2c). The 500–700 nm band present in the static measurements at 277K (Figure 2a) instead represents the $FADH^{\bullet}$ intermediate produced during the reduction of FAD^{ox} to $FADH^{-}$.

Using identical sample and experimental conditions from the UV-visible spectroscopy, we next applied difference FTIR spectroscopy to the redissolved sample of (6-4) PHR. Figure 3a shows the light-induced difference FTIR spectrum upon illuminating FAD^{ox} of (6-4) PHR at 450 nm. From the analysis in the UV-visible region (Figure 2a), the product is a mixture of 49 % $FADH^{\bullet}$ and 51 % $FADH^{-}$. Figure 3b represents the difference FTIR spectrum obtained by illuminating with >550-nm light, matching illumination conditions in Figure 2b. Therefore, Figure 3b corresponds to the $FADH^{-}$ minus $FADH^{\bullet}$ spectrum. The smaller amplitude in Figure 3b relative to that in Figure 3a probably results from photoconversion of half the $FADH^{\bullet}$. The red spectrum in Figure 3c is the sum of the two spectra in Figure 3a and b, which coincides very well with the $FADH^{-}$ minus FAD^{ox} spectrum (black line in Figure 3c) obtained by illuminating FAD^{ox} by the >450 nm light. Both spectra also coincide with the reported $FADH^{-}$ minus FAD^{ox} difference FTIR spectrum.[13]

Isolation of $FAD^{\bullet-}$: Light-Induced Difference UV-visible and FTIR Spectra of (6-4) PHR at 200 K

Conversion from FAD^{ox} to $FADH^{\bullet}$ occurs through both one-electron and one-proton transfer reactions. If only an electron transfer takes place, $FAD^{\bullet-}$ is produced from FAD^{ox}. The stability of this anion-radical is highly dependent on the protein environment. In particular, the amino acid nearest to the N_5 position of FAD is important.[15] In insect-specific CRY, functioning as the photoreceptor of the circadian clock, Cys near N_5 favors $FAD^{\bullet-}$ even at room temperature.[14] However, most PHR/CRY possess Asn or Asp, and typically stabilize $FADH^{\bullet}$ rather than $FAD^{\bullet-}$.[23] A hydrogen-bonding network anchored to FAD N_5 by Asn or Asp likely promotes efficient proton transfer. In *Synechocystis* CRY-DASH, another PHR homolog, mutation of the corresponding Asn to Cys stabilized $FAD^{\bullet-}$.[18] (6-4) PHRs also possess Asn at this position, and $FAD^{\bullet-}$ is not detected in *Xenopus* (6-4) PHR at room temperature (Figure 2), consistent with the previous reports.[13] However, one might expect separation of the electron and proton transfers by lowering temperature, and it was indeed the case.

At 200 K, the light-induced difference UV-visible spectrum (Figure 4) upon illuminating FAD^{ox} of (6-4) PHR exhibits a positive peak at ~380 nm, which is characteristic of the difference spectrum between $FAD^{\bullet-}$ and FAD^{ox}.[18] This spectrum indicates that $FAD^{\bullet-}$ is formed and stable in *Xenopus* (6-4) PHR at low temperature, but neither $FADH^{\bullet}$ nor $FADH^{-}$ accumulates. At 200 K, a broad positive feature is observable at 500-700 nm, yet the analysis in Figure S2 shows that, at most, the appearance of $FADH^{\bullet}$ is less than 5 %. Thus, the spectral feature at 500-700 nm cannot be explained by $FADH^{\bullet}$ alone (Figure S2), but likely indicates the involvement of cation or neutral radicals of Trp and/or Tyr in the positive side of Figure 4. The formation of a Trp cation radical visible at 200 K would be consistent with an important role for the tryptophan triad chain in the electron transfer reaction: if the farthest Trp is the electron donor to FAD, then the difference UV-visible spectrum (Figure 4) would contain the signal of Trp cation radical. Previous pulsed radiolysis studies reported that cation and neutral radicals of Trp show absorption maxima at 560 and 510 nm,[25] which are in good agreement with the positive spectral feature (Figure 4). The molar extinction coefficients of cation (ε_{510} = 2300 $M^{-1}cm^{-1}$) and neutral (ε_{560} = 3000 $M^{-1}cm^{-1}$) radicals of Trp are about 4–5 times smaller than that of FAD^{ox} in (6-4) PHR (ε_{450} = 11200 $M^{-1}cm^{-1}$).[9] Thus, low-temperature UV-visible spectroscopy might suggest the presence of the electron donor, possibly Trp from the triad. In contrast, in the case of *S*CRY-DASH, DTT was needed for the conversion from FAD^{ox} to $FAD^{\bullet-}$, where the broad positive feature at 500–700 nm was absent.[18] This observation strongly supports our interpretation. Since UV-visible difference spectroscopy established the experimental conditions for trapping $FAD^{\bullet-}$, we then apply FTIR spectroscopy at 200 K.

Light-Induced Difference FTIR Spectra of the Four Redox States of (6-4) PHR

Figure 5a corresponds to the $FAD^{\bullet-}$ minus FAD^{ox} difference FTIR spectrum measured at 200 K. Then, the $FADH^{\bullet}$ minus FAD^{ox} difference FTIR spectrum (Figure 5b) is obtained by subtracting the spectrum in Figure 3c from that in Figure 3a using the result of the UV-visible analysis (Figure 2a; 49 % $FADH^{\bullet}$ and 51 % $FADH^{-}$ as the product). The $FADH^{-}$ minus $FADH^{\bullet}$ difference FTIR spectrum in Figure 5c is reproduced from Figure 3b after

scaling the amplitude (divided by 0.49). The $FADH^-$ minus FAD^{ox} difference FTIR spectrum in Figure 5d is reproduced from Figure 3c. In this way, we are now able to obtain difference FTIR spectra among four redox states. It should be noted that, except for Figure 5c, the scale of the amplitude in Figure 5 is normalized for the FAD^{ox}-specific negative band at 1715 cm^{-1}.[13] The blue spectra in Figure 5 exhibit the identical measurements in D_2O.

Figure 5 shows that the bands at 1489, 1535, and 1397 cm^{-1} are specific to $FAD^{\bullet-}$, $FADH^{\bullet}$, and $FADH^-$, respectively, and can therefore be used as marker bands for future analysis. Frequencies of FAD^{ox} at 1715, 1690, 1578, and 1545 cm^{-1} (negative bands in Figure 5a, b, and d) are ascribable to the C_4=O, C_2=O, C_{4a}=N_5, and C_{10a}=N_1 stretching vibrations of flavin, respectively.[26–31] Previous theoretical study suggested that the 1625-cm^{-1} band of $FAD^{\bullet-}$ (Figure 5a) and the 1535-cm^{-1} band of $FADH^{\bullet}$ (Figure 5b) originate from C_2=O, and C_{10a}=N_1 stretching vibrations of flavin, respectively.[32,33] Thus, strong peaks are assignable for the vibrations of flavin, but vibrations of protein are possibly involved in the difference spectra as well.

Protonated Carboxylic COOH Stretching Vibrations at 1800-1700 cm^{-1}

C=O stretching vibrations of protonated carboxylic acids appear in the 1800-1700 cm^{-1} region, and are spectral downshifted by 5–15 cm^{-1} in D_2O.[34] Since there are no other vibrations in this region except for the C_4=O stretching vibration of flavin, detailed analysis of protonated carboxylic acids is possible. We observed only a negative peak at 1715 cm^{-1}, which shifted to 1714 cm^{-1} in D_2O (Figure 5a, b, and d). As mentioned, the FAD^{ox} specific band originates from the C_4=O stretching vibration of isoalloxazine ring.[26] Lack of other bands indicates that there are no structural changes for protonated carboxylic acids among four redox states. It should be noted that one proton is gained by the flavin from FAD^{ox}/$FAD^{\bullet-}$ to $FADH^{\bullet}$/$FADH^-$. A protonated carboxylic acid is a good candidate for the proton donor, and in fact, for photoreduction of plant CRY, a negative FTIR band at 1735 cm^{-1} suggested that a carboxylic acid is the FAD proton donor.[35] Unlike plant CRY, in the case of (6-4) PHR, protonated carboxylic acid is not the proton donor.[13] Consistent with the FTIR results, plant CRY anchors the redox-active FAD N_5 position with a hydrogen bond to the carboxylic acid Asp,[36] whereas PHRs conserve this position as Asn.[5]

Involvement of Trp and/or Tyr: the Frequency Region at 1500-1000 cm^{-1}

If Trp in the triad is the electron donor for the formation of $FAD^{\bullet-}$, the $FAD^{\bullet-}$ minus FAD^{ox} difference FTIR spectrum at 200 K (Figure 5a) also contains the vibrations of $Trp^{\bullet+}$ in the positive side and Trp in the negative side. Previous theoretical calculations of indolyl radical cation suggested the presence of the normal modes at 1459, 1074, and 1040 cm^{-1},[37] Thus, the positive peaks at 1489, 1060, and 1046 cm^{-1} in Figure 5a are good candidates for $Trp^{\bullet+}$ vibrations that can be tested by isotopic labeling in the future.

A common peak pair in Figure 5 is observed at 1227 (−)/1215 (+) cm^{-1}, which is upshifted by 3–5 cm^{-1}, not downshifted, in D_2O. When Tyr functions as both a hydrogen-bond donor and acceptor, Tyr vibration exhibits such a characteristic feature for H/D exchange[38]. The frequency change at 200 K for the $FAD^{\bullet-}$ minus FAD^{ox} difference FTIR spectrum (Figure

5a), indicates that this change accompanies the primary electron transfer. The peak pair at 1227 (−)/1215 (+) cm^{-1} is similarly observed in the $FADH^{\bullet}$ minus FAD^{ox} difference FTIR spectrum (Figure 5b), but the amplitude is smaller (0.46-times of Figure 5a). This suggests that the structural change, possibly owing to Tyr, is partially relaxed by the subsequent proton transfer. The peak pair is also observed in the $FADH^{-}$ minus $FADH^{\bullet}$ difference FTIR spectrum in Figure 5c, whose amplitude is even smaller (0.39-times of Figure 5a). As the consequence, the amplitude of the peak pair in the $FADH^{-}$ minus FAD^{ox} difference FTIR spectrum (Figure 5d) is 0.85-times of Figure 5a. From these results, two Tyr may be involved in the photoactivation reaction, where both change their hydrogen-bonding structures from FAD^{ox} to $FAD^{\bullet-}$, but neither is an electron donor. Upon formation of $FADH^{\bullet}$, the structure of one Tyr is preserved, while the other is restored. Then, $FADH^{-}$ formation changes the structures of two Tyr again. If instead a Tyr radical was formed, its signal would appear at ~1500 cm^{-1}.[39,40] Since this signature band of the Tyr radical is not present in these spectra (Figure 5a–d), the data instead provide support for our alternative interpretation.

Secondary Structure Perturbations at 1700-1600 cm^{-1}

Amide-I, the C=O stretching vibration of the peptide backbone, appears in this frequency region.[41] The unique spectral features are obtained for each difference FTIR spectrum, and the enlarged spectra are shown in Figure S3. It should be noted that this region contains other vibrations such as those of flavin and/or side chains of proteins. In general, amide-I is little influenced by H/D exchange, and the spectral downshift by >3 cm^{-1} in D_2O does not originate from amide-I. For instance, the bands at 1688 (−), 1672 (+), and 1666 (+) cm^{-1} in the $FAD^{\bullet-}$ minus FAD^{ox} difference FTIR spectrum (Figure 5a) do not originate from amide-I, but those at 1633 (−), and 1625 (+) cm^{-1} may contain amide-I vibrations. Previous study showed that the bands at 1688 (−), and 1625 (+) cm^{-1} originates from the C_2=O stretching vibration for FAD^{ox} and $FAD^{\bullet-}$, respectively.[32] Therefore, the positive band at 1625 cm^{-1} mainly originates from the C_2=O stretching vibration of flavin. However, from the presence of the peak pair at 1633 (−) and 1625 (+) cm^{-1}, and the small H/D effect for the negative band at 1633 cm^{-1}, it is possible that the $FAD^{\bullet-}$ minus FAD^{ox} difference FTIR spectrum contains the amide-I vibration at these frequencies. The peak pair at 1633 (−)/1625 (+) cm^{-1} is characteristic of the amide-I vibration of β-sheet conformation.

The $FADH^{\bullet}$ minus FAD^{ox} difference FTIR spectrum (Figure 5b) shows the negative band at 1690 cm^{-1}, which is most likely to be the C_2=O stretch of FAD.[13,26] Also, previous study showed that the twin positive peaks at 1663 and 1654 cm^{-1} should be contained the C_2=O stretching vibration for $FADH^{\bullet}$.[32] On the other hand, twin positive peaks at 1663 and 1654 cm^{-1} are insensitive for H/D exchange, though their amplitudes were considerably decreased. Therefore, the bands probably originate from amide-I vibrations, with a frequency characteristic of α-helical conformation.[38] Thus, the primary electron transfer ($FAD^{\bullet-}$ formation) is accompanied by structural perturbation of the β-sheet, and the subsequent proton transfer ($FADH^{\bullet}$ formation) increases α-helical conformation.

Figure 5c apparently shows that the $FADH^{-}$ minus $FADH^{\bullet}$ difference FTIR spectrum is highly sensitive to H/D exchange. Nevertheless, it should be noted that the spectral

featuresare similar between H_2O and D_2O. The negative peak at 1661 cm^{-1} is largely reduced in D_2O, but the amplitude of the peak pairs at 1661 (−)/1645 (+) cm^{-1} in H_2O and at 1661 (−)/1643 (+) cm^{-1} in D_2O are similar. This suggests the amide-I origin, and the apparent decrease of the negative 1661-cm^{-1} band in D_2O may be due to the baseline drift. The positive peak at 1625 cm^{-1} looks H/D unexchangeable, though the amplitude is decreased. Amide-I changes are more clearly observable in D_2O. Since amide-I vibrations at 1660–1650 cm^{-1} and 1640-1620 cm^{-1} are characteristic of α-helix and β-sheet, respectively, the secondary electron transfer ($FADH^-$ formation) accompanies structural changes that decrease α-helical conformation and enhance β-strand conformation in (6-4) PHR. These secondary structural changes of the protein backbone need not be in the same region.

In summary, the primary electron transfer ($FAD^{\bullet-}$ formation) is accompanied by structural perturbation of the β-sheet, but no significant changes in α-helicity. The subsequent proton transfer ($FADH^{\bullet}$ formation) causes a transient increase in α-helicity. Secondary structural rearrangement of an α-helix or α-helices may be needed for the proton uptake to FAD. Subsequently, the final electron transfer ($FADH^-$ formation) is accompanied by decreased α-helicity and increase β-strand conformation. As the consequence, when we compare the fully oxidized (FAD^{ox}) and reduced ($FADH^-$) states, there are no changes in α-helicity, but significant perturbations in β-sheet conformation.

Structural Similarity of $FAD^{\bullet-}$ and $FADH^-$

Figure 6 compares the $FAD^{\bullet-}$ minus FAD^{ox} (red line) and the $FADH^-$ minus FAD^{ox} (black line) spectra, which are reproduced from Figure 5. As is clearly seen, the two spectra are similar, including amide-I vibration. This implies structural similarity between $FAD^{\bullet-}$ and $FADH^-$, whose chemical structures of FAD are different, but both carry negative charge. The $FAD^{\bullet-}$ specific band at 1489 cm^{-1} and $FADH^-$ specific band at 1397 cm^{-1} presumably originate from FAD. Previous study suggested that the bands at 1489 (+), and 1397 (+) cm^{-1} originate from the C=N stretching vibration, and in-plane rocking mode for N_5-H, respectively.[32,42]

In the amide-I region, there are common positive peaks at 1674, 1665, 1652, and 1625 cm^{-1} for both $FAD^{\bullet-}$ and $FADH^-$. This observation together with different amide-I signals for $FADH^{\bullet}$ and FAD^{ox} (Figure 5b) strongly suggests that the negative charge at the chromophore is important for the structure of (6-4) PHR. In other words, the protein structures of four redox states in (6-4) PHR can be classified into three confomations; FAD^{ox}, $FADH^{\bullet}$, and $FAD^{\bullet-}$/$FADH^-$.

Spectral Comparison between (6-4) PHR and CRY-DASH

Despite striking similarities among homologous members of the CRY/PHR family, their functional diversity remains puzzling. We previously reported the $FAD^{\bullet-}$ minus FAD^{ox}, and the $FADH^-$ minus FAD^{ox} spectra of the DASH-type cryptochrome from *Synechocystis* (CRY-DASH).[18] Since we now have the difference FTIR spectra of the four redox states of *Xenopus* (6-4) PHR, it is intriguing to compare these spectra with those of CRY-DASH. Figure 7 shows overlaid $FAD^{\bullet-}$ minus FAD^{ox} (a) and $FADH^-$ minus FAD^{ox} (b) FTIR spectra for (6-4) PHR (black line) and CRY-DASH (green line).

Negative FAD^{ox} specific peaks at 1715, 1690, 1578 and 1545 cm^{-1} are common between *Xenopus* (6-4) PHR and *S*CRY-DASH, and ascribable for the C_4=O, C_2=O, C_{4a}=N_5, and C_{10a}=N_1 stretching vibrations of FAD, respectively.[26–31] Similarly, the $FAD^{\bullet-}$ specific peak at 1489 cm^{-1} for (6-4) PHR is commonly observed for *S*CRY-DASH (Figure 7a), while the $FADH^-$ specific peak at 1396 cm^{-1} is commonly observed for both (Figure 7b). These bands probably originate from the flavin chromophore, and common peaks for each redox state are reasonable.[18]

In contrast to the conservation of chromophore bands between the CRY-DASH and (6-4) PHR, the protein bands are different. The peak pair at 1227 (−)/1215 (+) cm^{-1} for (6-4) PHR, possibly owing to Tyr, which was not clearly observable for *S*CRY-DASH. In Raman data of *Vibrio* cryptochrome1, another type of CRY-DASH, however, the 1227 cm^{-1} band characteristic of $FADH^{\bullet}$ was observed.[43] This suggests that *S*CRY-DASH does not contain the corresponding Tyr residue. On the basis of sequence and three-dimensional analysis, the possible candidates for the Tyr residues in (6-4) PHR are Y254, Y295, Y296 and Y412.[4,5] To identify the signal, further experiments, such as mutation analysis, are required, however, these tyrosines are located 4-8 Å from FAD and are not present in the *S*CRY-DASH sequence.

Prominent spectral difference can be seen in the amide-I region between (6-4) PHR and CRY-DASH. In the case of CRY-DASH, a negative peak at 1663 cm^{-1}, observed for the $FAD^{\bullet-}$ minus FAD^{ox}, and the $FADH^-$ minus FAD^{ox} spectra (green curve in Figure 7), is unexchangeable for D_2O.[18] This strongly suggests structural perturbation of α-helicity upon formation of $FAD^{\bullet-}$ and $FADH^-$ from FAD^{ox} in CRY-DASH, but not in (6-4) PHR. For the $FAD^{\bullet-}$ state, the 1609-cm^{-1} band for CRY-DASH is much lower in frequency than for (6-4) PHR (1625 cm^{-1}). For the $FADH^-$ state, the peaks at 1675, 1647, 1627, and 1601 cm^{-1} are all insensitive to H/D exchange,[18] and thus assignable for amide-I vibration. These results suggest that protein structural changes are larger in CRY-DASH than in (6-4) PHR, and this might reflect the functional difference between sensor and enzyme.

DISCUSSION

There are four different redox states for the FAD chromophore of PHR; a fully oxidized form (FAD^{ox}), an anion radical form ($FAD^{\bullet-}$), a neutral radical form ($FADH^{\bullet}$) and a fully reduced form ($FADH^-$). The enzymatically active state of PHR is $FADH^-$, and two photons are needed for the activation: FAD^{ox} is first converted to $FADH^{\bullet}$ by light-induced one electron and one proton transfers and then to $FADH^-$ by light-induced one electron transfer. In this paper, we studied the detailed activation process of *Xenopus* (6-4) PHR using UV-visible and FTIR spectroscopy. By lowering the temperature (200 K), we successfully trapped $FAD^{\bullet-}$, where electron transfer occurs, but proton transfer does not. We then observed $FADH^{\bullet}$ after the subsequent proton transfer reaction by the 450-nm illumination at 277 K, where the $FADH^-$ signal in the difference FTIR spectra could be deconvoluted, by using the results from UV-visible spectroscopy. We finally obtained the $FAD^{\bullet-}$ minus FAD^{ox}, the $FADH^{\bullet}$ minus FAD^{ox}, and the $FADH^-$ minus FAD^{ox} spectra, from which any difference spectrum among the four redox states can be calculated. Detailed structural analysis requires band assignments using isotope-labeling and site-directed mutagenesis, as

we performed for bacteriorhodopsin[44,45] and LOV domain,[46,47] while we discuss the molecular mechanism on the activation of (6-4) PHR based on the present FTIR results below.

Environment of the Flavin Chromophore in (6-4) PHR

Light-induced difference FTIR spectra contain signals from both chromophore and protein. In general, the former is predominant, as has been shown for retinal proteins[48] and LOV domains,[49,50] and is also the case for (6-4) PHRs and CRYs. Frequencies of FAD^{ox} at 1715, 1690, 1578, and 1545 cm^{-1} (negative bands in Figure 5a, b, and d) can be assigned to the C_4=O, C_2=O, C_{4a}=N_5, and C_{10a}=N_1 stretching vibrations of flavin, respectively.[26–31] The bands at 1489, 1535, and 1397 cm^{-1}, being specific to $FAD^{\bullet-}$, $FADH^{\bullet}$, and $FADH^{-}$, respectively, are also ascribable to vibrations of the flavin chromophore. The 1489-cm^{-1} band of $FAD^{\bullet-}$ possibly originates from the C=N stretching vibrations in the isoalloxazine ring,[32] while ring vibration of $Trp^{\bullet+}$ may also be involved.[37] Previous theoretical study suggested that the 1625-cm^{-1} band of $FAD^{\bullet-}$ (Figure 5a) originates from C_2=O stretching vibration of flavin. Recent theoretical calculation of lumiflavin (LF) reported that the ring vibration mainly consisting of C=N stretches in isoalloxazine (1545 cm^{-1}) is slightly downshifted in the neutral radical ($LFH^{\bullet}$), while being split into two differently down-shifted and much weaker bands in anion radical ($LF^{\bullet-}$).[32] Therefore, the band at 1535 cm^{-1} is ascribable for C=N stretching vibration in $FADH^{\bullet}$. The H/D unexchangeable band at 1397 cm^{-1} of $FADH^{-}$, possibly originates from ring vibrations of the flavin chromophore.[51] In fact, this band is observed for $FADH^{-}$ of CRY-DASH (Figure 7). Thus, in the CRY/PHR family, the strong FTIR peaks are assignable to flavin vibrations. Similar frequencies for FAD between solution and protein environments suggest that the structural properties of the flavin chromophore are maintained in (6-4) PHR.

Electron and Proton Transfer Reactions in (6-4) PHR

Photoactivation of (6-4) PHR is accompanied by electron and proton transfer processes distinct from DNA repair reaction. The primary electron transfer converts FAD^{ox} into $FAD^{\bullet-}$, followed by a proton transfer to form $FADH^{\bullet}$, and finally $FADH^{-}$ is formed by the secondary electron transfer. There must be two electron donors and one proton donor for activation from FAD^{ox}, whereas none of them has been identified for (6-4) PHR. Regarding the primary electron transfer, important role of the tryptophan triad chain has been suggested. In the case of *E. coli* CPD PHR, substitution of the farthest Trp of the triad chain disturbs the electron transfer,[7] and (6-4) PHRs structurally conserve the tryptophan triad chain with some modification. Presence of visible absorption at 500–700 nm (Figure 4) and FTIR bands at 1489, 1060, and 1046 cm^{-1} (Figure 5a) suggests the involvement of radical species, possibly $Trp^{\bullet+}$.

One proton is gained to flavin in the conversion from $FAD^{\bullet-}$ to $FADH^{\bullet}$. Successful isolation of the primary electron transfer and proton transfer at 200 K implies that the proton transfer is accompanied by conformational changes in the protein. Protonated carboxylic acids are good candidates for the proton donor to the FAD, and in fact, a negative FTIR band observed at 1735 cm^{-1} suggested that a carboxylic acid is the FAD proton donor for photoreduction of plant CRY.[35] However, Figure 5 shows the absence of such bands for

(6-4) PHR, indicating that protonated carboxylic acid is not the proton donor. Consistent with the FTIR results, plant CRY anchors the redox-active FAD N_5 position with a hydrogen bond to the carboxylic acid Asp,[35] whereas PHRs conserve this position as Asn.[5] At present, the proton donor and secondary electron donor to FAD in (6-4) PHR remain to be identified. It should be noted that unlike other CRY/PHR family members including CRY-DASH, (6-4) PHR can form $FADH^-$ stably without a reducing agent such as DTT, implying that light energy is sufficient to exceed the potential barrier for forming $FADH^-$. Although the identification of the proton and secondary electron donors await futher investigation, the present FTIR spectra provide the analytical basis of future study.

Secondary Structural Changes during the Activation of (6-4) PHR

The structure of (6-4) PHR has a typical CRY/PHR fold, consisting of an N-terminal α/β domain and a C-terminal α-helical domain, containing the active-site FAD. Our spectral analysis of the amide-I vibration reveals that the primary electron transfer ($FAD^{\bullet-}$ formation) in *Xenopus* (6-4) PHR is accompanied by perturbation of the β-sheet conformation, but no significant changes in α-helicity. The subsequent proton transfer ($FADH^{\bullet}$ formation) causes a transient increase in α-helicity that is reversed by the secondary electron transfer ($FADH^-$ formation), which also enhances β-sheet conformation. As the consequence, when we compare fully oxidized (FAD^{ox}) and reduced ($FADH^-$) states, there are no significant changes for α-helicity, but more noticeable perturbation for β-sheet conformation. Small changes in α-helicity in (6-4) PHR may be characteristic of activation of this enzyme.

Relatively small structural changes for (6-4) PHR are supported by the spectral resemblance between the $FAD^{\bullet-}$ minus FAD^{ox} (200 K) and $FADH^-$ minus FAD^{ox} (277 K) difference FTIR spectra (Figure 6). At 200 K, protein structural changes are limited compared to higher temperatures, whereas similar spectra, particularly on the amide-I bands, suggest local structural perturbation around the FAD chromophore. Lack of the signal in α-helix for (6-4) PHR, unlike CRY-DASH, in Figure 7 may also support this argument. In the previous paper, we compared the $FADH^-$ minus FAD^{ox} spectra in the absence and presence of oligonucleotides containing the (6-4) photoproduct.[13] Although the two spectra were very similar, we reported an additional negative peak at 1653 cm^{-1} only in the presence of the damaged DNA. This suggests that structural perturbation takes place only in the DNA-bound form of (6-4) PHR. The spectral analysis for the photoactivation in the presence of (6-4) photoproduct is thus intriguing. In addition, one might expect the possibility that $FAD^{\bullet-}$ could have the DNA repair activity, because of the structural similarity between $FAD^{\bullet-}$ and $FADH^-$.

CONCLUSION

We examined different FAD redox states of (6-4) PHR by UV−visible and FTIR spectroscopy, and successfully obtained difference FTIR spectra among four redox states of FAD. Spectral analysis of the C=O stretching vibration of protonated carboxylic acids shows the lack of the signal upon proton transfer reaction, implying that carboxylic acids are not proton donor. Involvement of structural changes in Trp and Tyr is suggested from the UV-

visible and FTIR analysis of $FAD^{\bullet -}$. The spectral analysis of amide-I vibration reveals that the primary electron transfer ($FAD^{\bullet -}$ formation) is accompanied by perturbation of the β-sheet conformation, but not α-helicity. The subsequent proton transfer ($FADH^{\bullet}$ formation) causes a transient increase in α-helicity that is reversed by the secondary electron transfer ($FADH^{-}$ formation), which also perturbs the β-sheet conformation. On the basis of the obtained difference FTIR spectra, isotope-labeling and various mutants of (6-4) PHR will provide a detailed molecular mechanism for the photoactivation of this enzyme.

Supplementary Material

Refer to Web version on PubMed Central for supplementary material.

REFERENCES

1. Sancar A. Structure and function of DNA photolyase and cryptochrome blue-light photoreceptors. Chem. Rev. 2003; 103:2203–2237. [PubMed: 12797829]
2. Weber S. Light-driven enzymatic catalysis of DNA repair: a review of recent biophysical studies on photolyase. Biochim. Biophys. Acta. 2005; 1707:1–23. [PubMed: 15721603]
3. Todo T, Takemori H, Ryo H, Ihara M, Matsunaga T, Nikaido O, Sato K, Nomura T. A new photoreactivating enzyme that specifically repairs ultraviolet light-induced (6-4) photoproducts. Nature. 1993; 361:371–374. [PubMed: 8426655]
4. Maul MJ, Barends TR, Glas AF, Cryle MJ, Domratcheva T, Schneider S, Schlichting I, Carell T. Crystal structure and mechanism of a DNA (6-4) photolyase. Angew. Chem. Int. Ed. 2008; 47:10076–10080.
5. Hitomi K, DiTacchio L, Arvai AS, Yamamoto J, Kim ST, Todo T, Tainer JA, Iwai S, Panda S, Getzoff ED. Functional motifs in the (6-4) photolyase crystal structure make a comparative framework for DNA repair photolyases and clock cryptochromes. Proc. Natl. Acad. SciU.SA. 2009; 106:6962–6967.
6. Hitomi K, Kim ST, Iwai S, Harima N, Otoshi E, Ikenaga M, Todo T. Binding and catalytic properties of *Xenopus* (6-4) photolyase. J. Biol. Chem. 1997; 272:32591–32598. [PubMed: 9405474]
7. Aubert C, Vos MH, Mathis P, Eker AP, Brettel K. Intraprotein radical transfer during photoactivation of DNA photolyase. Nature. 2000; 405:586–590. [PubMed: 10850720]
8. Kim ST, Li YF, Sancar A. The third chromophore of DNA photolyase: Trp-277 of Escherichia coli DNA photolyase repairs thymine dimers by direct electron transfer. Proc. Natl. Acad. SciU.SA. 1992; 89:900–904.
9. Todo T, Kim ST, Hitomi K, Otoshi E, Inui T, Morioka H, Kobayashi H, Ohtsuka E, Toh H, Ikenaga M. Flavin adenine dinucleotide as a chromophore of the Xenopus (6-4) photolyase. Nucleic Acids Res. 1997; 25:764–768. [PubMed: 9016626]
10. Kandori H. Role of internal water molecules in bacteriorhodopsin. Biochim. Biophys. Acta. 2000; 1460:177–191. [PubMed: 10984599]
11. Kötting C, Gerwert K. Proteins in action monitored by time-resolved FTIR spectroscopy. ChemPhysChem. 2005; 6:881–888. [PubMed: 15884070]
12. Noguchi T. Light-induced FTIR difference spectroscopy as a powerful tool toward understanding the molecular mechanism of photosynthetic oxygen evolution. Photosynth. Res. 2007; 91:59–69. [PubMed: 17279438]
13. Zhang Y, Iwata T, Yamamoto J, Hitomi K, Iwai S, Todo T, Getzoff ED, Kandori H. FTIR study of light-dependent activation and DNA repair processes of (6-4) photolyase. Biochemistry. 2011; 50:3591–3598. [PubMed: 21462921]
14. Berndt A, Kottke T, Breitkreuz H, Dvorsky R, Hennig S, Alexander M, Wolf E. A novel photoreaction mechanism for the circadian blue light photoreceptor*Drosophila* cryptochrome. J. Biol. Chem. 2007; 282:13011–13021. [PubMed: 17298948]

15. Kao Y-T, Tan C, Song S-H, Öztürk N, Li J, Wang L, Sancar A, Zhong D. Ultrafast dynamics and anionic active states of the flavin cofactor in cryptochrome and photolyase. J. Am. Chem. Soc. 2008; 130:7695–7701. [PubMed: 18500802]
16. Öztürk N, Song S-H, Selby CP, Sancer A. Animal type 1 cryptochromes. J. Biol. Chem. 2008; 283:3256–3263. [PubMed: 18056988]
17. Hitomi K, Okamoto K, Daiyasu H, Miyashita H, Iwai S, Toh H, Ishiura M, Todo T. Bacterial cryptochrome and photolyase: characterization of two photolyase-like genes of *Synechocystis* sp. PCC6803. Nucleic Acids Res. 2000; 28:2353–2362. [PubMed: 10871367]
18. Iwata T, Zhang Y, Hitomi K, Getzoff ED, Kandori H. Key dynamics of conserved asparagine in a cryptochrome/photolyase family protein by Fourier transform infrared spectroscopy. Biochemistry. 2010; 49:8882–8891. [PubMed: 20828134]
19. Zhang Y, Yamamoto J, Yamada D, Iwata T, Hitomi K, Todo T, Getzoff ED, Iwai S, Kandori H. Substrate assignment of the (6-4) photolyase reaction by FTIR spectroscopy. J. Phys. Chem. Lett. 2011; 2:2774–2777.
20. Iwata T, Yamamoto A, Tokutomi S, Kandori H. Hydration and temperature similarly affects light-induced protein structural changes in the chromophore domain of phototropin. Biochemistry. 2007; 46:7016–7021. [PubMed: 17503781]
21. Yamamoto A, Iwata T, Tokutomi S, Kandori H. Role of Phe1010 in light-induced structural changes of the neo1-LOV2 domain of *Adiantum* . Biochemistry. 2008; 47:922–928. [PubMed: 18163650]
22. Schleicher E, Hitomi K, Kay CWM, Getzoff ED, Todo T, Weber S. Electron nuclear double resonance differentiates complementary roles for active site histidines in (6-4) photolyase. J. Bio. Chem. 2007; 282:4738–4747. [PubMed: 17164245]
23. Langenbacher T, Immeln D, Dick B, Kottke T. Microsecond light-induced proton transfer to flavin in the blue light sensor plant cryptochrome. J. Am. Chem. Soc. 2009; 131:14274–14280. [PubMed: 19754110]
24. Offenbacher AR, Vassiliev IR, Seyedsayamdost MR, Stubbe J, Barry BA. Redox-linked structural changes in ribonucleotide reductase. J. Am. Chem. Soc. 2009; 131:7496–7497. [PubMed: 19489635]
25. Solar S, Surdhar NGPS, Armstrong DA, Singh A. Oxldatlon of tryptophan and N-methylindole by $N_3^{\bullet}$, Br_2^{-}, and $(SCN)_2^{-}$ radlcals in light-and Heavy-Water Solutions: A pulse radiolysis study. J. Phys. Chem. 1991; 95:3639–3643.
26. Wille G, Ritter M, Friedemann R, Möntele W, Hübner G. Redox-triggered FTIR difference spectra of FAD in aqueous solution and bound to flavoproteins. Biochemistry. 2003; 42:14814–14821. [PubMed: 14674755]
27. Bowman WD, Spiro TG. Normal mode analysis of lumiflavin and interpretation of resonance Raman spectra of flavoproteins. Biochemistry. 1981; 20:3313–3318. [PubMed: 7248286]
28. Schmidt J, Coudron P, Thompson AW, Watters KL, McFarland JT. Assignment and the effect of hydrogen bonding on the vibrational normal modes of flavins and flavoproteins. Biochemistry. 1983; 22:76–84. [PubMed: 6830765]
29. Abe M, Kyogoku Y. Vibrational analysis of flavin derivatives: normal coordinate treatments of lumiflavin. Spectrochim. Acta. 1987; 43 A:1027–1038.
30. Livery CR, McFarland JT. Assignment and the effect of hydrogen bonding on the vibrational normal modes of flavins and flavoproteins. J. Phys. Chem. 1990; 94:3980–3994.
31. Zhang W, Vivoni A, Lombard JR, Birke RL. Time-resolved SERS study of direct photochemical charge transfer between FMN and a Ag electrode. J. Phys. Chem. 1995; 99:12846–12857.
32. Rieff B, Bauer S, Mathias G, Tavan P. IR spectra of flavins in solution: DFT/MM description of redox effects. J. Phys. Chem. B. 2011; 115:2117–2123. [PubMed: 21309580]
33. Li J, Uchida T, Ohta T, Todo T, Kitagawa T. Characteristic structure and environment in FAD cofactor of (6-4) photolyase along function revealed by resonance Raman spectroscopy. J. Phys. Chem. B. 2006; 110:16724–16732. [PubMed: 16913812]
34. Barth A. The infrared absorption of amino acid side chains. Progress Biophys. Mol. Biol. 2000; 74:141–173.

35. Kottke T, Batschauer A, Ahmad M, Heberle J. Blue-light-induced changes in Arabidopsis cryptochrome 1 probed by FTIR difference spectroscopy. Biochemistry. 2006; 45:2472–2479. [PubMed: 16489739]
36. Brautigam CA, Smith BS, Ma Z, Palnitkar M, Tomchick DR, Machius M, Deisenhofer J. Structure of the photolyase-like domain of cryptochrome 1 from Arabidopsis thaliana. Proc. Natl. Acad. SciU.SA. 2004; 101:12142–12147.
37. Walden SE, Wheeler RA. Structural and vibrational analysis of indolyl radical and indolyl radical cation from density functional methods. J. Chem. Soc. Perkin Trans. 1996; 2:2663–2672.
38. Takahashi R, Okajima K, Suzuki H, Nakamura H, Ikeuchi M, Noguchi T. FTIR study on the hydrogen bond structure of a key tyrosine residue in the flavin-binding blue light sensor TePixD from. Thermosynechococcus elongates. 2007; 46:6459–6467.
39. Berthomieu C, Boussac A. FTIR and EPR study of radical of aromatic amino acids 4-methylimidazole and phenol generated by UV irradiation. Biospectroscopy. 1995; 1:187–206.
40. Noguchi T, Inoue Y, Tang XS. Structural coupling between the oxygen-evolving Mn cluster and a tyrosine residue in photosystem II as revealed by fourier transform infrared spectroscopy. Biochemistry. 1997; 36:14705–14711. [PubMed: 9398190]
41. Krimm S, Bandekar J. Vibrational spectroscopy and conformation of peptides, polypeptides, and proteins. Adv. Protein Chem. 1986; 38:181–364. [PubMed: 3541539]
42. Schleicher E, Hessling B, Illarionova V, Bacher A, Weber S, Richter G, Gerwert K. Light-induced reactions of Escherichia coli DNA photolyase monitored by Fourier transform infrared spectroscopy. FEBS. J. 2005; 272:1855–1866. [PubMed: 15819881]
43. Sokolowsky K, Newton M, Lucero C, Wertheim B, Freedman J, Cortazar F, Czochor J, Schelvis JPM, Gindt YM. Spectroscopic and Thermodynamic Comparisons of Escherichia coli DNA Photolyase and Vibrio cholerae Cryptochrome 1. J. Phys. Chem. B. 2010; 114:7121–7130. [PubMed: 20438097]
44. Kandori H, Kinoshita N, Yamazaki Y, Maeda A, Shichida Y, Needleman R, Lanyi JK, Bizounok M, Herzfeld J, Raap J, Lugtenburg J. Local and distant protein structural changes on photoisomerization of the retinal in bacteriorhodopsin. Proc. Natl. Acad. Sci. USA. 2000; 97:4643–4648. [PubMed: 10758159]
45. Tanimoto T, Shibata M, Belenky M, Herzfeld J, Kandori H. Altered hydrogen bonding of Arg82 during the proton pump cycle of bacteriorhodopsin: A low-temperature polarized FTIR spectroscopic study. Biochemistry. 2004; 43:9439–9447. [PubMed: 15260486]
46. Iwata T, Nozaki D, Sato Y, Sato K, Nishina Y, Shiga K, Tokutomi S, Kandori H. Identification of the C=O stretching vibrations of FMN and peptide backbone by 13C-labeling of the LOV2 domain of Adiantum phytochrome3. Biochemistry. 2006; 45:15384–15391. [PubMed: 17176060]
47. Koyama T, Iwata T, Yamamoto A, Sato Y, Matsuoka D, Tokutomi S, Kandori H. Different role of the Ja helix in the light-induced activation of the LOV2 domains in various phototropins. Biochemistry. 2009; 48:7621–7628. [PubMed: 19601589]
48. Siebert F. Infrared spectroscopy applied to biochemical and biological problems. Methods Enzymol. 1995; 246:501–526. [PubMed: 7752935]
49. Kottke T, Hegemann P, Dick B, Heberle J. The photochemistry of the light-, oxygen-, and voltage-sensitive domains in the algal blue light receptor phot. Biopolymers. 2006; 82:373–378. [PubMed: 16552739]
50. Iwata T, Tokutomi S, Kandori H. Light-induced structural changes of the LOV2 domains in various phototropins revealed by FTIR spectroscopy. BIOPHYSICS. 2011; 7:89–98.
51. Zheng Y, Carey PR, Palfey BA. Raman spectrum of fully reduced flavin. J. Raman Spectrosc. 2004; 35:521–524.

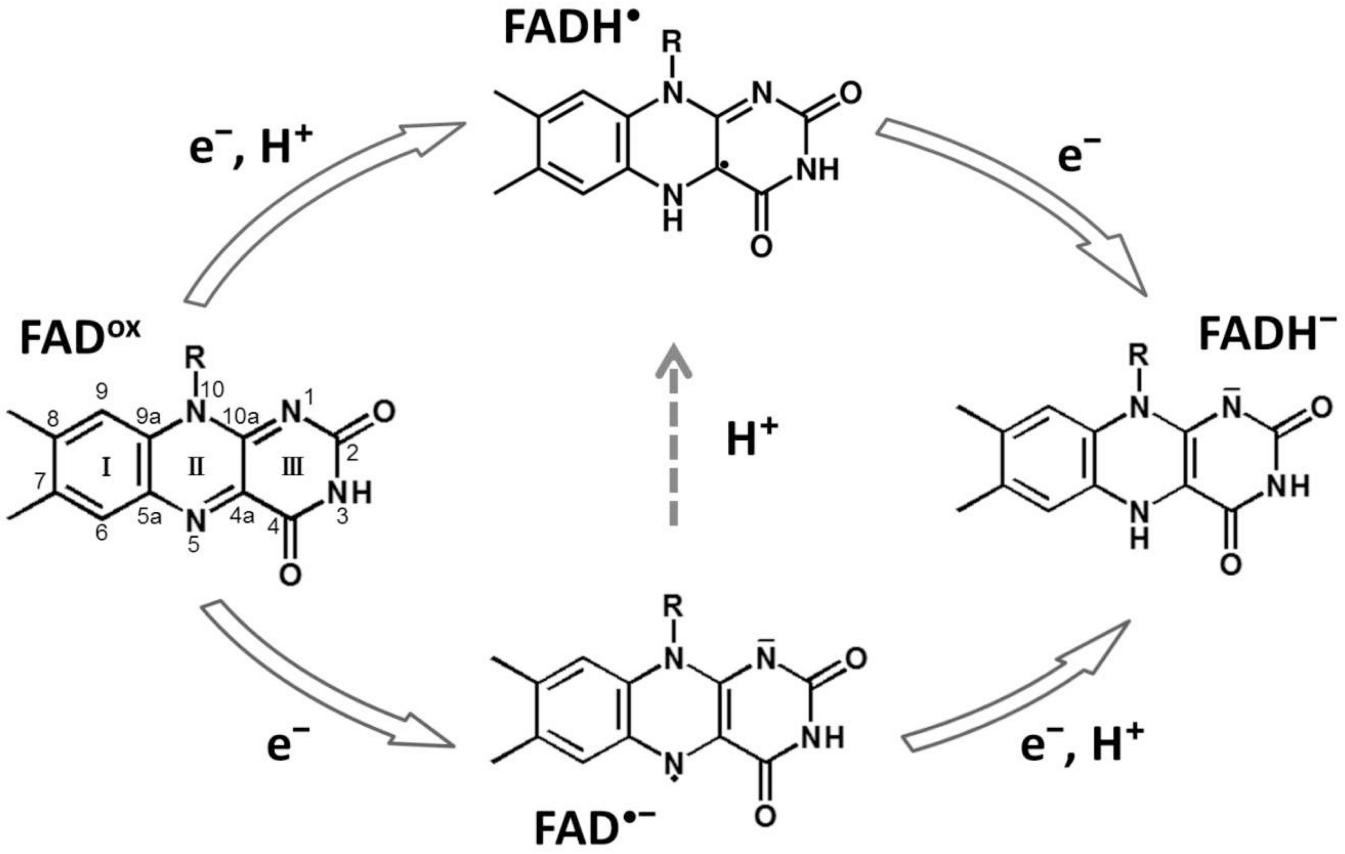

Figure 1.

Four redox states of FAD in the CRY/PHR family. An oxidized form (FAD^{ox}) is the most stable species in *Xenopus* (6-4) PHR, insect CRY, and CRY-DASH from *Synechocystis* (*S*CRY-DASH). For activation of *Xenopus* (6-4) PHR, FAD^{ox} is first converted to a neutral radical form ($FADH^{\bullet}$) by light-induced one electron and one proton transfers (upper pathway) and then into a fully reduced form ($FADH^{-}$) by light-induced one electron transfer (upper pathway).[1] In insect CRY, FAD^{ox} is converted to an anion radical form ($FAD^{\bullet -}$) by light-induced one electron transfer (lower pathway), and $FAD^{\bullet -}$ is highly stable.[14] In *S*CRY-DASH, FAD^{ox} is first converted to $FAD^{\bullet -}$ by light-induced one electron transfer (lower pathway), and then into a fully reduced form ($FADH^{-}$) by light-induced one electron and one proton transfer (lower pathway).[18]

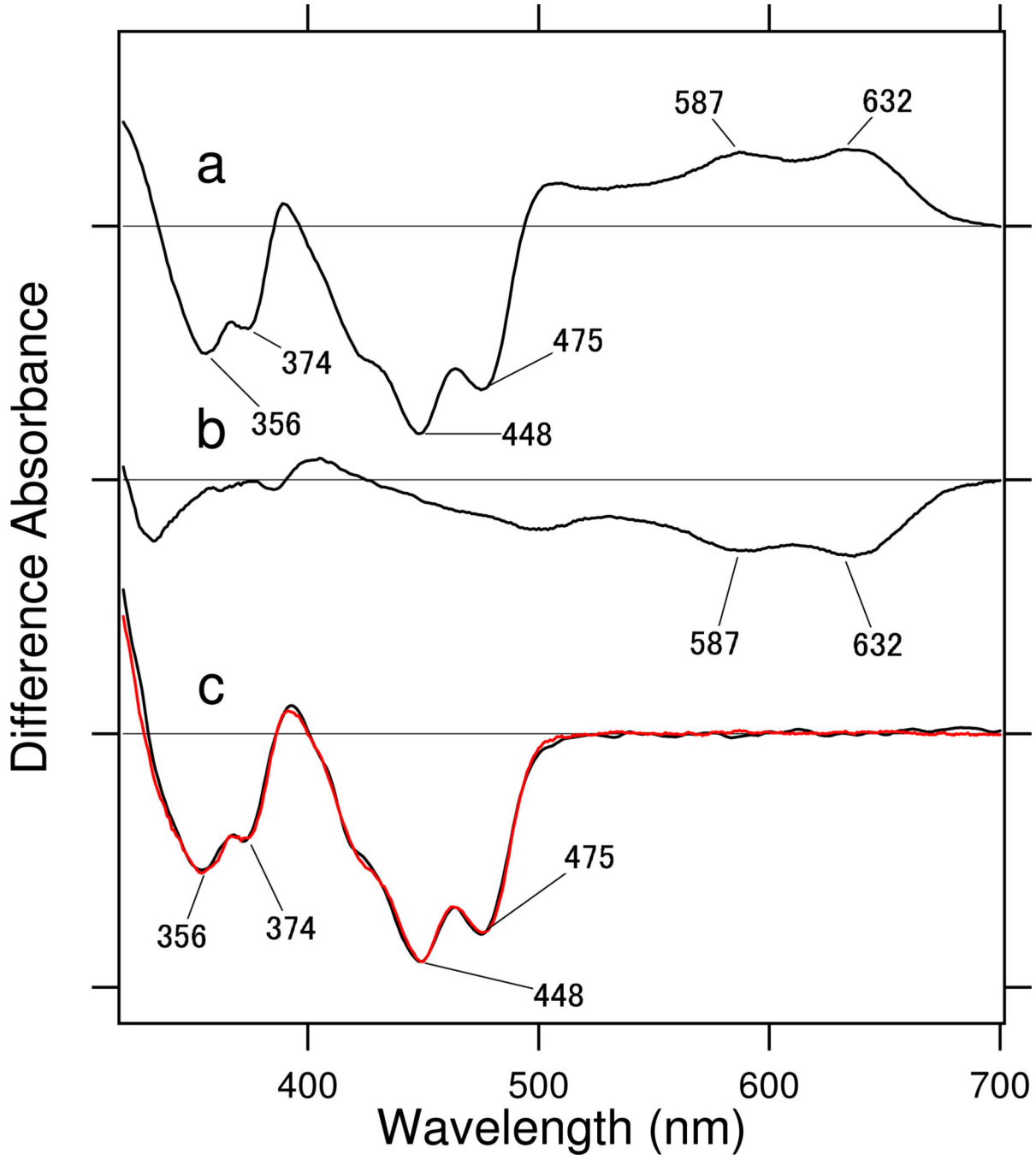

Figure 2.

Light-induced difference UV-visible spectra of the redissolved sample of *Xenopus* (6-4) PHR at 277 K. (a) Difference spectrum by a 450-nm light illumination (an interference filter) of FAD^{ox} for 4 min, where $FADH^{\bullet}$ is formed as shown by broad positive absorption at 500-700 nm. Note that $FADH^{-}$ is also produced under these illumination conditions, and the relative amounts of $FADH^{\bullet}$ and $FADH^{-}$ produced are estimated to be 0.49 and 0.51, respectively, by using their individual molar extinction coefficients (see text). (b) After the illumination in Figure 2a, the sample is illuminated at >550 nm light for 1 min, which

provides the $FADH^-$ minus $FADH^\bullet$ difference spectrum. (c) The sum of (a) and (b) (red line) coincides with the $FADH^-$ minus FAD^{ox} difference spectrum obtained by illumination of FAD^{ox} at >450 nm for 4 min (black line). One division of the *y*-axis corresponds to 0.04 absorbance units.

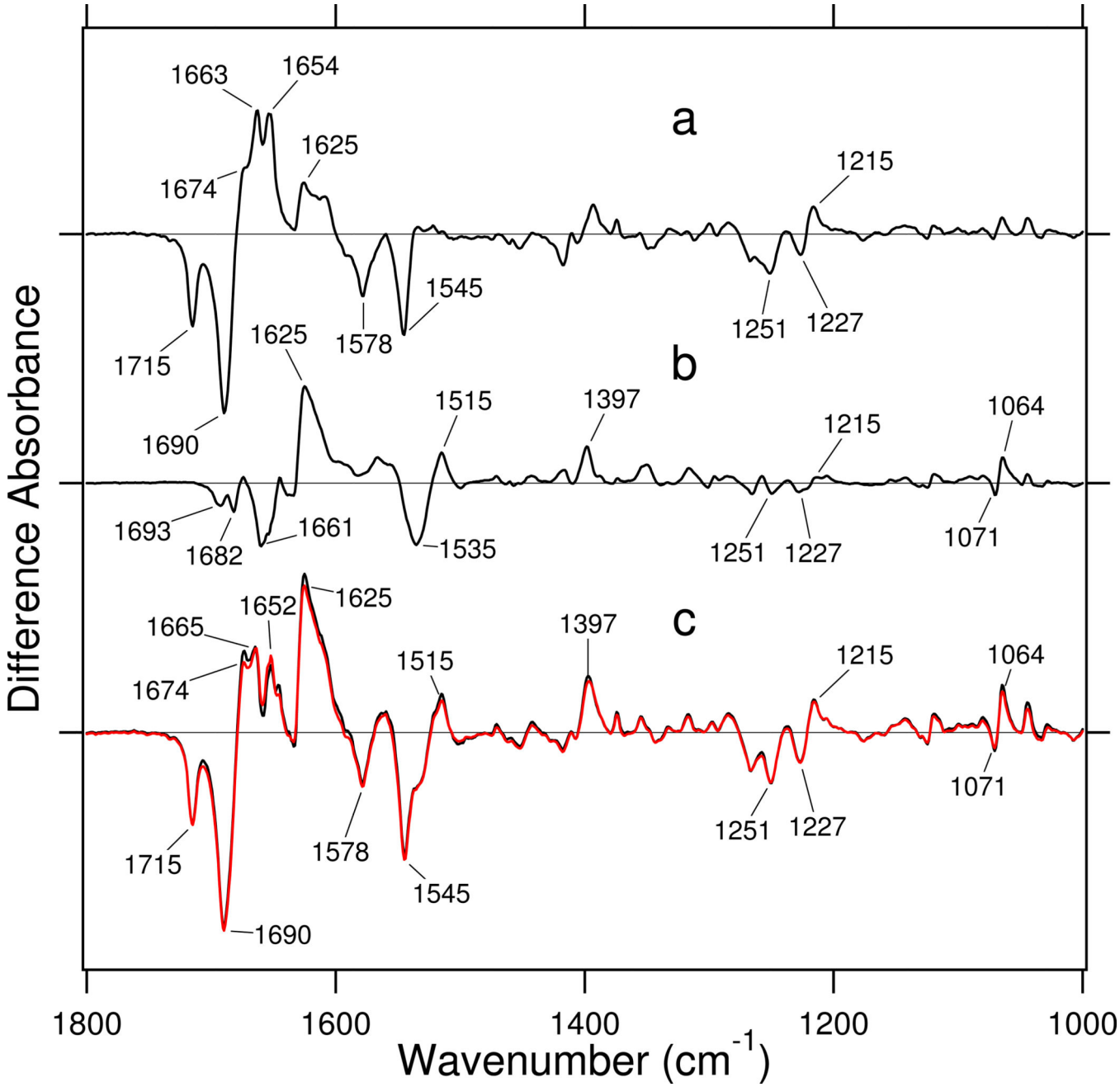

Figure 3.

Light-induced difference FTIR spectra of the redissolved sample of *Xenopus* (6-4) PHR at 277 K. (a) Difference spectrum by a 450-nm light illumination (an interference filter) of FAD^{ox} for 4 min (identical condition to Figure 2a), where the product is 49 % $FADH^{\bullet}$ and 51 % $FADH^{-}$. (b) After the illumination in Figure 3a, the sample is illuminated at >550 nm light for 1 min (identical condition to Figure 2b), which provides the $FADH^{-}$ minus $FADH^{\bullet}$ difference spectrum. (c) The sum of (a) and (b) (red line) coincides with the $FADH^{-}$ minus FAD^{ox} difference spectrum obtained by illumination of FAD^{ox} at >450 nm for 4 min (black line). One division of the *y*-axis corresponds to 0.008 absorbance units.

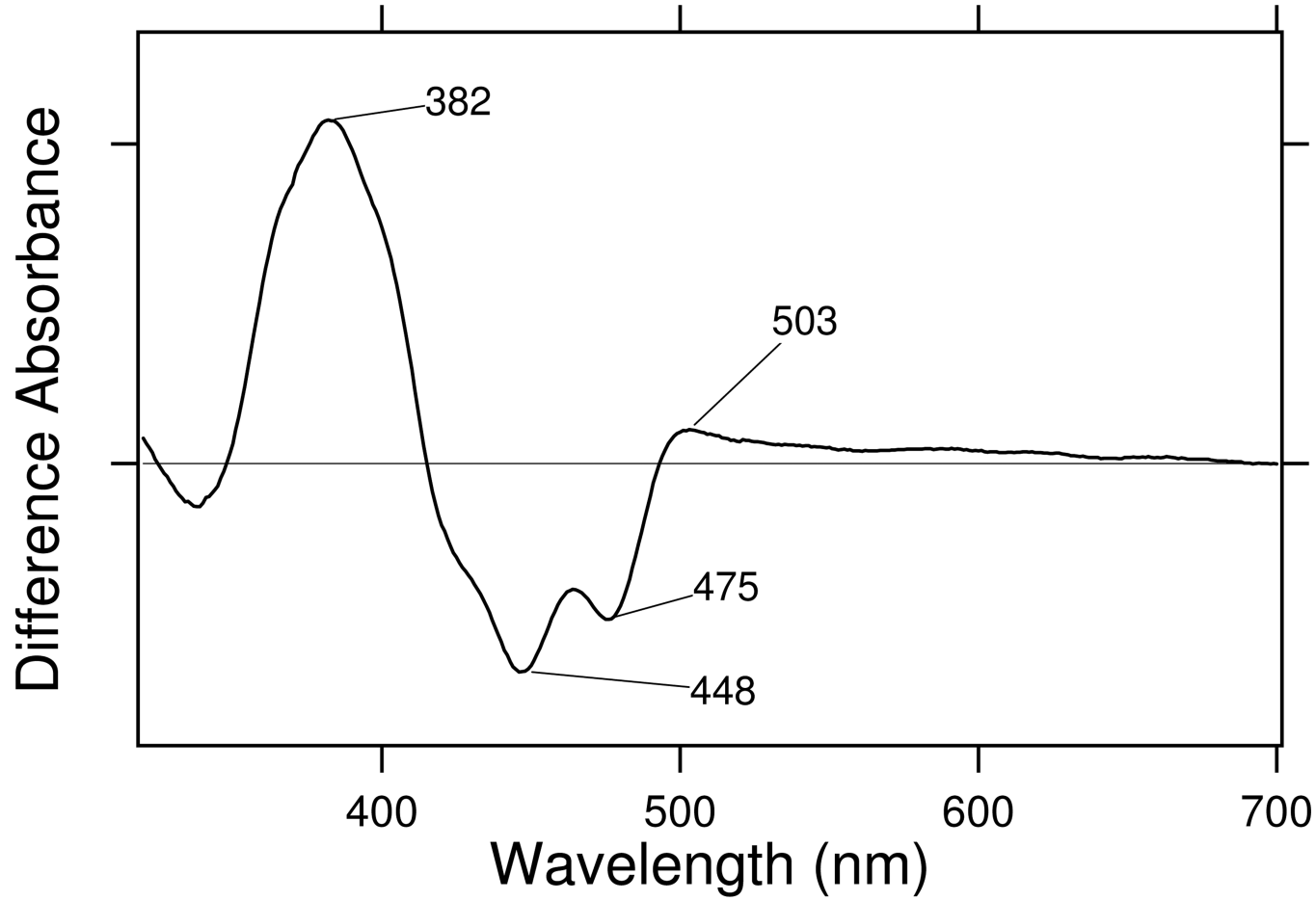

Figure 4.

Light-induced difference UV-visible spectra of the redissolved sample of *Xenopus* (6-4) PHR at 200 K. FAD^{ox} is illuminated by a 300–400 nm light for 20 min, whose difference spectrum is entirely different from Figure 2a. A positive peak is characteristic of the formation of $FAD^{\bullet -}$. One division of the *y*-axis corresponds to 0.015 absorbance units.

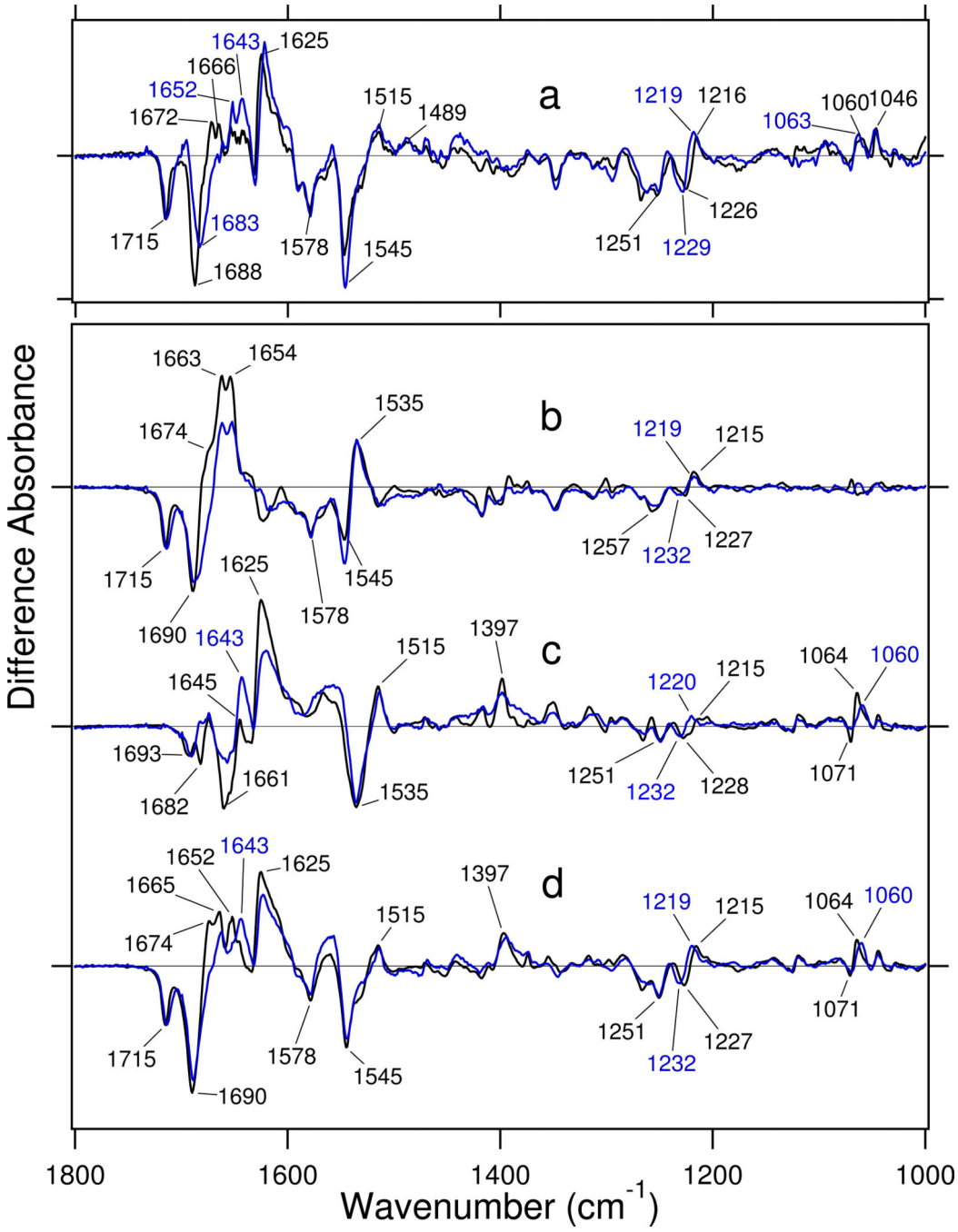

Figure 5.

Light-induced difference FTIR spectra of the redissolved sample of *Xenopus* (6-4) PHR in H_2O (black line) and D_2O (blue line). (a) FAD^{ox} is illuminated by a 300–400 nm light for 20 min at 200 K (identical condition to Figure 4), and light-minus-dark difference spectra correspond to the $FAD^{\bullet -}$ minus FAD^{ox} spectra. The obtained spectra are magnified by 4.05 times, so that the negative band at 1715 cm^{-1} exhibits the same amplitude to that in the $FADH^-$ minus FAD^{ox} spectrum (Figure 5d). (b) The $FADH^{\bullet}$ minus FAD^{ox} spectra calculated from those in Figure 3a and 3c (black line) so as to remove the contribution of

FADH$^-$ (see text). The calculated spectra are magnified by 2.04 times, so that the negative band at 1715 cm^{-1} exhibits the same amplitude to that in the FADH$^-$ minus FAD^{ox} spectrum (Figure 5d). (c) The FADH$^-$ minus FADH$^\bullet$ spectra reproduced from Figure 3b, but the amplitude was magnified by 2.04 times so as to show the same molar reaction. (d) The FADH$^-$ minus FAD^{ox} spectra reproduced from the black line in Figure 3c. From the normalizations shown above, Figure 5a–d show the same molar reaction with each other. One division of the *y*-axis corresponds to 0.0065 (above) or 0.012 (below) absorbance units.

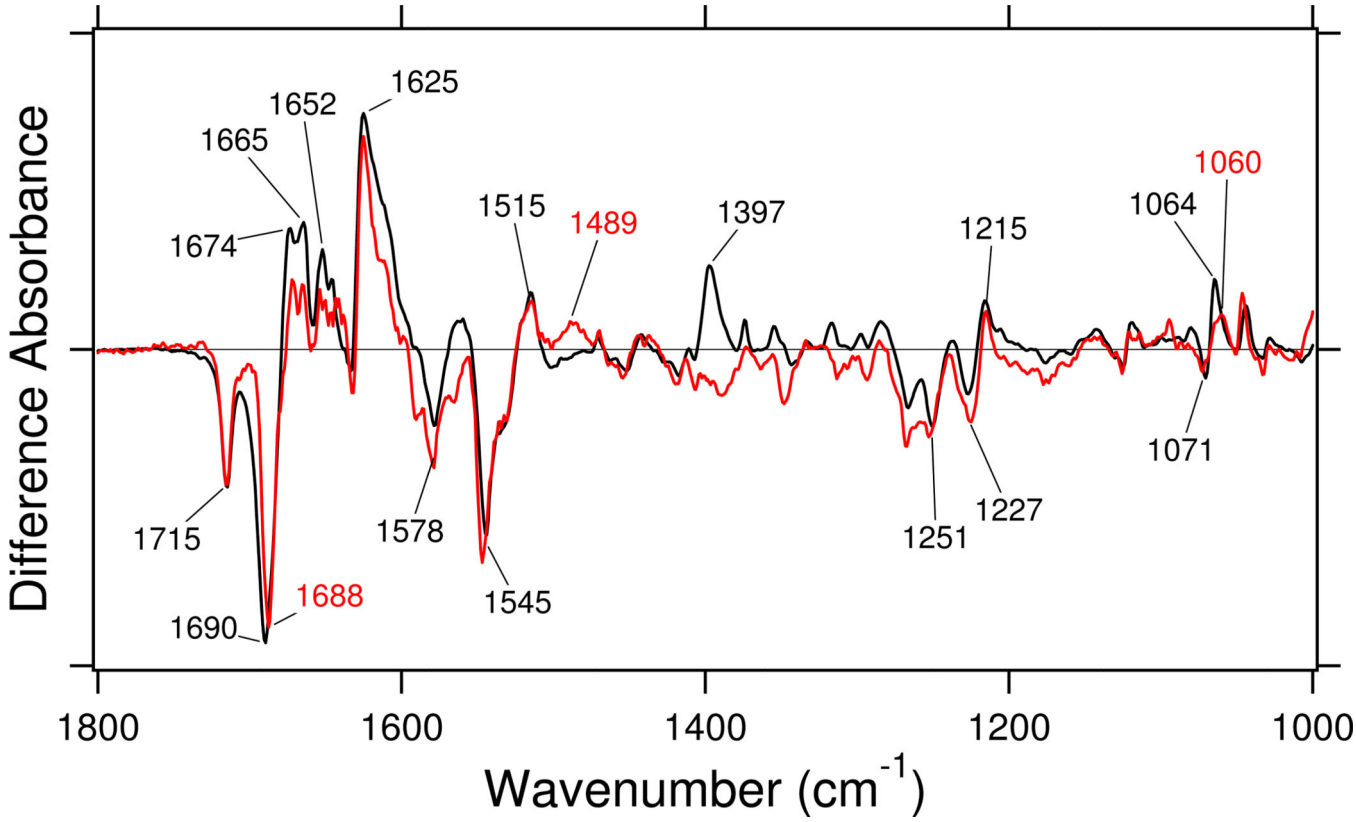

Figure 6.

Comparison of the $FAD^{\bullet -}$ minus FAD^{ox} (red line), and $FADH^{-}$ minus FAD^{ox} (black line) difference FTIR spectra of *Xenopus* (6-4) PHR, which are reproduced from the black lines in Figure 5a and d, respectively.

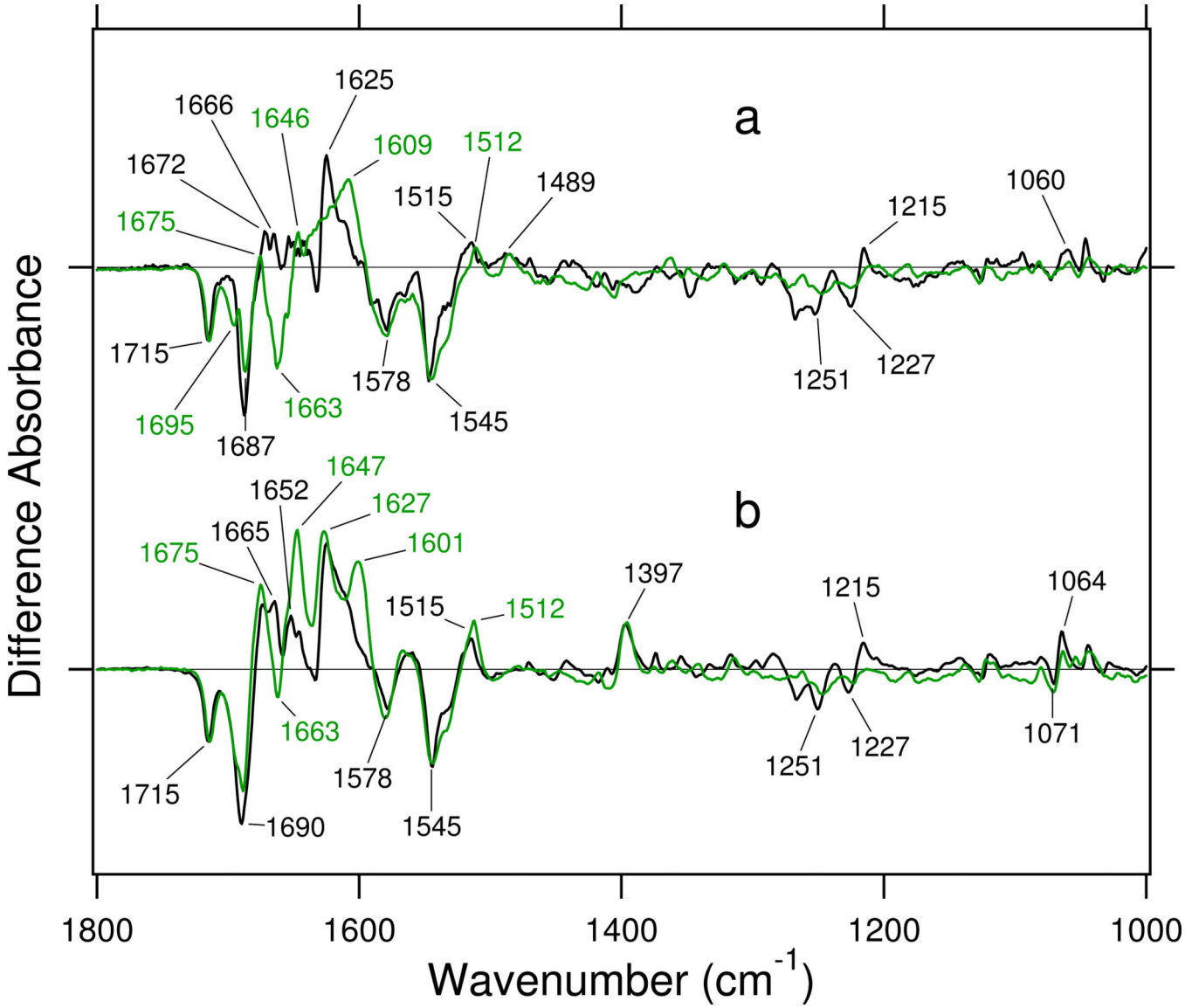

Figure 7.

Comparison of light-induced difference FTIR spectra of *Xenopus* (6-4) PHR (black lines) and *S*CRY-DASH (green lines). (a) The $FAD^{\bullet -}$ minus FAD^{ox} difference FTIR spectra. (b) The $FADH^{-}$ minus FAD^{ox} difference FTIR spectra.